11th Australasian Fluid Mechanics Conference
University of Tasmania, Hobart, Australia
14-18 December 1992

VORTICAL FLOW COMPUTATIONS ON A FLEXIBLE BLENDED WING-BODY COMBINATION

Guru P. GURUSWAMY

Computational Aerosciences Branch
NASA Ames Research Center
Moffett Field, CA 94035-1000, USA

ABSTRACT

Flows over blended wing-body configurations are often dominated by vortices. The unsteady aerodynamic forces due to such flows can couple with the elastic forces of the wing and lead to aeroelastic oscillations. Such aeroelastic oscillations can impair the performance of an aircraft. In order to study this phenomenon, it is necessary to account for structural properties of the configuration, and solve the aerodynamic and aeroelastic equations of motion simultaneously. In this work, the flow is modeled using the Navier-Stokes equations coupled with the aeroelastic equations of motion. Computations are made for a blended wing-body configuration at flow conditions dominated by vortices and separation. The computed results are validated with the available experimental data. Almost sustained aeroelastic oscillations observed in the wind tunnel are successfully simulated for $M_\infty = 0.975$, $\alpha \approx 8.0$ deg and a frequency of about 2Hz.

INTRODUCTION

To date, most of the calculations for wings with vortical flows have been restricted to steady and unsteady computations on rigid wings. However, to accurately compute such flows, it is necessary to account for the wing's flexibility. The aeroelastic deformation resulting from this flexibility can considerably change the nature of the flow. Strong interactions between the vortical flows and the structures can lead to sustained aeroelastic oscillations for highly swept wings(Dobbs and Miller, 1985). In order to compute the flows accurately, it is necessary to include both aerodynamic and structural effects of the body. In this work, the flow is modeled using the Navier-Stokes equations coupled with the aeroelastic equations of motion for blended wing-body configurations.

The computer code developed for computing the unsteady aerodynamics and aeroelasticity of aircraft by using the Navier-Stokes equations is referred to as ENSAERO (Guruswamy, 1990). The code has the capability to compute aeroelastic responses by simultaneously integrating the Navier-Stokes equations and the modal structural equations of motion, using aeroelastically adaptive dynamic grids. In this work, computations are presented for vortical-flow conditions about a flexible blended wing-body configuration and the results are compared with the available experiments. The formation of vortices and their effects on the aeroelastic responses are demonstrated.

GOVERNING AERODYNAMIC EQUATIONS

The strong conservation law form of the Navier-Stokes equations are used for shock capturing purposes. The thin-layer version of the equations in generalized coordinates can be written as

$$\partial_\tau \hat{Q} + \partial_\xi \hat{E} + \partial_\eta \hat{F} + \partial_\zeta \hat{G} = Re^{-1} \partial_\zeta \hat{S} \quad (1)$$

where $\hat{Q}, \hat{E}, \hat{F}, \hat{G}$, and $\hat{S}$, are flux vectors in generalized coordinates.

In this paper, the central-difference scheme based on the diagonalizied version of the implicit approximate factorization algorithm (Beam and Warming ,1976) is used along with an algebraic eddy-viscosity model by Baldwin and Lomax (1978).

AEROELASTIC EQUATIONS OF MOTION

It is assumed that the deformed shape of the wing can be represented by a set of discrete displacements at selected nodes. From the modal analysis, the displacement vector $\{d\}$ can be expressed as $[\phi]\{q\}$ where $[\phi]$ is the modal matrix and $\{q\}$ is the generalized displacement vector.

The final matrix form of the aeroelastic equations of motion is

$$[M]\{\ddot{q}\} + [G]\{\dot{q}\} + [K]\{q\} = \{Z\} \quad (2)$$

where [M], [G], and [K] are modal mass, damping, and stiffness matrices, respectively. $\{Z\}$ is the aerodynamic force vector defined as $(\frac{1}{2})\rho U_\infty^2 [\phi]^T [A]\{\Delta C_p\}$ and $[A]$ is the diagonal area matrix of the aerodynamic control points.

The aeroelastic equation of motion, Eq. (2), is solved by a numerical integration technique based on the linear acceleration method by Guruswamy and Yang (1980). Aeroelastic configuration adaptive moving grids are used for the computations (Guruswamy, 1990,1991).

RESULTS

To validate the present development, computations were made for a blended wing-body configuration shown in Fig. 1. For this configuration, aerodynamic and aeroelastic experimental data are given by Dobbs and Miller (1985). From the results on aeroelastic damping versus the angle of attack (Dobbs and Miller, 1985) show that the configuration undergoes limit cycle oscillations at $M_\infty = 0.975$, $Re_c = 6$ million, and $\alpha \approx 8.0$ deg. At other angles of attack the configuration is dynamically stable. It was observed in the experiment that the configuration experienced oscillations predominantly in the first bending mode. Hence, this oscillation is not associated with the conventional bending-torsion flutter. Earlier investigation based on the computations made using an inviscid transonic small perturbation code led to the possibilities of aeroelastic oscillations associated with vortices. This phenomenon

is further investigated in this paper by using the Navier-Stokes results with a turbulence model.

In this paper computations are presented at two flow conditions for which detailed data were available to author from the wind-tunnel tests. First, computations are shown at $M_\infty = 0.805$, $Re_c = 7.5$ million, and $\alpha = 10.5$ deg at which there are no aeroelastic oscillations. Next, computations are shown at $M_\infty = 0.975$, $Re_c = 6$ million, and for $\alpha = 0.0$, 8.0, and 12.0 deg. These cases are selected since at $\alpha \approx 8.0$ deg the configuration experienced aeroelastic oscillations.

The wing-body configuration shown in Fig. 1 is modeled using a C-H type grid of size 151 x 40 x 40. Figure 2 shows the density contours at $M_\infty = 0.805$, $Re_c = 7.5$ million, and $\alpha = 10.5$ deg. Figure 2 shows that the flow is dominated by the presence of a strong vortex on the wing and the flow is separated near the tip. The presence of the vortex on the wing can be seen at 50% and 75% wing semispan stations. The computed pressures compared fairly well with those measured in the wind tunnel (Guruswamy, 1991). The wing tip deflected by about 5% of the root chord due to aerodynamic loads. The same order of deflection was observed in the wind-tunnel tests. These calculations confirm the validity of the grid and aeroelastic modeling of the configuration.

The body portion of this configuration is rigid and the wing portion is flexible. The modal data required for the aeroelastic analysis is computed for six modes by the finite element method. Figure 3 shows the mode shapes and frequencies of the first four normal modes for the current configuration. This modal data compares well with the measured data. By using the normal modal data shown in Fig. 3, aeroelastic responses were computed by simultaneously integrating the flow equation (Eq. 1) and the aeroelastic equation (Eq. 2) in ENSAERO. Freestream conditions are used as initial conditions for the flow. The wing is started from a rigid steady-state position. Aeroelastic responses are computed at $M_\infty = 0.975$, $Re_c = 6$ million and angles of attack of 0.0, 8.0 and 12.0 deg. The dynamic pressure is set to 1.60 psi, which corresponds to that used in the wind tunnel to simulate flight conditions at an altitude of 32,000 feet.

The steady state density contours at three angles of attack of 0.0, 8.0, and 12.0 deg. are shown in Fig. 4. From Fig. 4 it can be seen that vortices on the wing are present at angles of attack of 8.0 and 12.0 deg. The flow begins to separate at $\alpha = 8.0$ deg and is fully separated at $\alpha = 12.0$ deg. As a result of flow separation, the vortex near the tip is lifted off the wing for $\alpha = 12.0$ deg. This leads to lower sectional lift near the tip.

For all angles of attack, the equations of motion are integrated for 12500 time steps which corresponds to a physical time of 3.0 seconds. Figure 5 shows the unsteady sectional lift coefficients for three angles of attack at the root. Since the wing is rigidly fixed to the root, fluctuations in the lift near the root are small. The fluctuations in lift increase towards the tip because of the wing's flexibility. These fluctuations have two main components, one due to the aeroelastic oscillations of the wing and the other due to the unsteadiness in the flow. It is noted here that the flow unsteadiness is initiated by an initial disturbance given to the structure. The fluctuations for $\alpha = 0.0$ deg is only due the aeroelastic oscillations. For angles of attack of 8.0 and 12.0 deg, the fluctuations contain components from both aeroelastic oscillations and flow unsteadiness. The contribution of flow unsteadiness to the fluctuations is greater for the $\alpha = 8.0$ deg case than for $\alpha = 12.0$ deg case. This can be seen in Fig. 5, particularly at the 75% semispan station. It is also noticed that the magnitude of the lift for $\alpha = 12.0$ deg is smaller than that for $\alpha = 8.0$ deg at the 75% semispan station. The reduction in both the magnitude and unsteadiness of the lift at 12.0 deg is due to a weaker interaction between the wing movement and vortex. One possible reason for such weaker interaction at $\alpha = 12.0$ deg is the presence of a thicker boundary layer on which the vortex rides during the oscillations.

Figure 6 shows the responses of the first mode for all three angles of attack. The response at $\alpha = 8.0$ deg has less damping than the responses at $\alpha = 0.0$ and 12.0 deg. At $\alpha = 8.0$ deg, the flow unsteadiness has strongly influenced the aeroelastic responses. The acceleration response in Fig. 6 shows the high frequency oscillations due to the flow unsteadiness for $\alpha = 8.0$ deg. The damping for $\alpha = 8.0$ deg is approaching zero as time reaches 3 seconds. This was further confirmed by continuing the integration for 2 more seconds. A Fourier analysis is conducted on the lift responses to further investigate the cause for these aeroelastic oscillations. The results from the Fourier analysis are shown for the 75% semispan section in Fig. 7. This plot shows that most of the contribution from flow unsteadiness is concentrated near the low frequencies around 2Hz and high frequencies around 14Hz. The energy contribution of the flow at low frequencies near 2Hz has lead to almost sustained aeroelastic oscillations. It is noted that the wing oscillated in the wind tunnel at a frequency of about 2Hz. More details about this work can be found in the AIAA paper by the author (1991).

CONCLUSIONS

Based on the present computations, the following explanation can be given for the phenomenon. At $\alpha = 0.0$ deg the flow is fully attached and free from vortices. Based on the classical flutter theory, the swept wing is stable at these conditions. At $\alpha = 8.0$ deg the flow is dominated by the presence of a strong vortex on the wing with small amounts of flow separation near the tip. The presence of a strong vortex leads to higher suction pressure on the wing. At these conditions, there is a strong interaction between the structure and the flow. Since the flow is very sensitive to any disturbance, it is highly unsteady. As a result, any small disturbance leads to almost sustained aeroelastic oscillations. At $\alpha = 12.0$ deg, the flow is fully separated and the boundary layer becomes thick. As a result, there is a weak interaction between the structure and flow which quickly damps out disturbance.

REFERENCES

BEAM, R. and WARMING, R F (1976) An Implicit Finite-Difference Algorithm for Hyperbolic Systems in Conservation Law Form. J of Computational Physics 22, 87-110.

BALDWIN, BS and LOMAX, H (1978) Thin-Layer Approximation and Algebraic Model for Separated Turbulent Flows. AIAA Paper 78-257.

DOBBS, SK and MILLER, GD (1985) Self Induced Oscillation Wind Tunnel Test of a Variable Sweep Wing. AIAA Paper 85-0739, AIAA Structural Dynamics Conf. Orlando, Florida.

GURUSWAMY, G and YANG, TY (1980) Aeroelastic Time Response Analysis of Thin Airfoils by Transonic Code LTRAN2. Computers and Fluids, 9, 409-425.

GURUSWAMY, GP (1990) ENSAERO-A Multidisciplinary Program for Fluid/Structural Interaction Studies of Aerospace Vehicles. Computing Systems in Engg. 237-256.

GURUSWAMY, GP (1991) Vortical Flow Computations on a Flexible Blended Wing-Body Configuration. AIAA-91-1013. 32nd Structural Dynamics Conf. Baltimore, Maryland, 719-734.

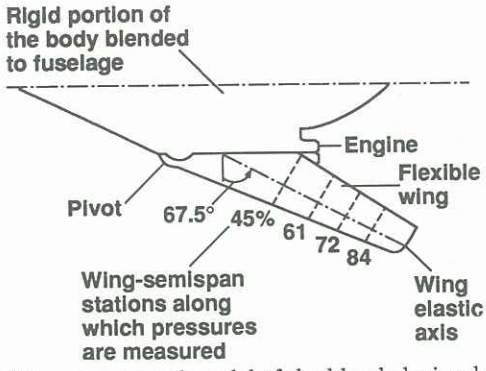

Fig. 1 The wind-tunnel model of the blended wing-body configuration.

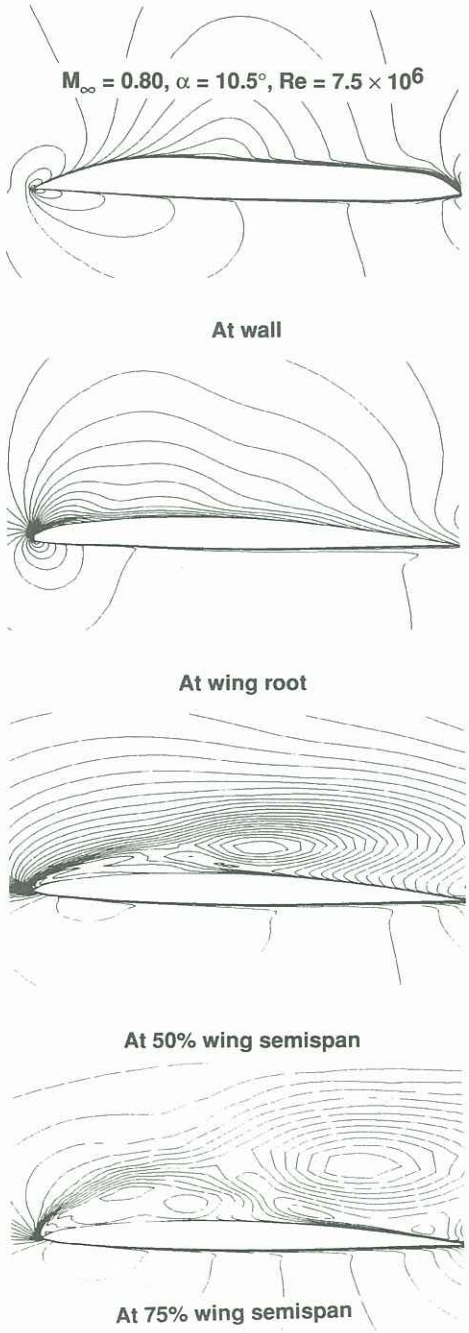

Fig. 2 Density contours on the aeroelastically deformed configuration.

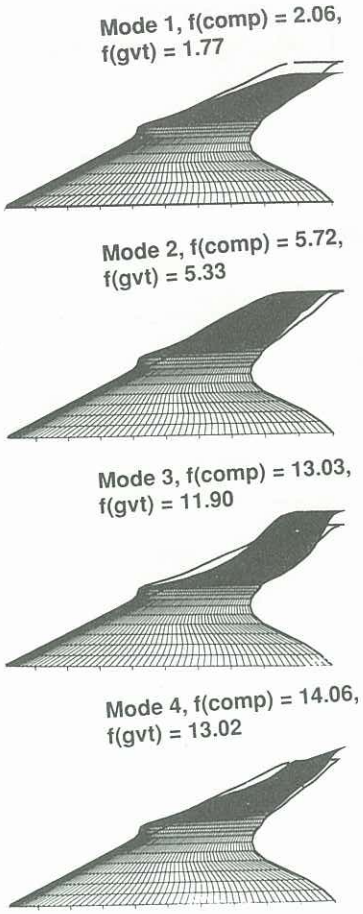

Fig. 3 Structural modes of wing-body configuration.

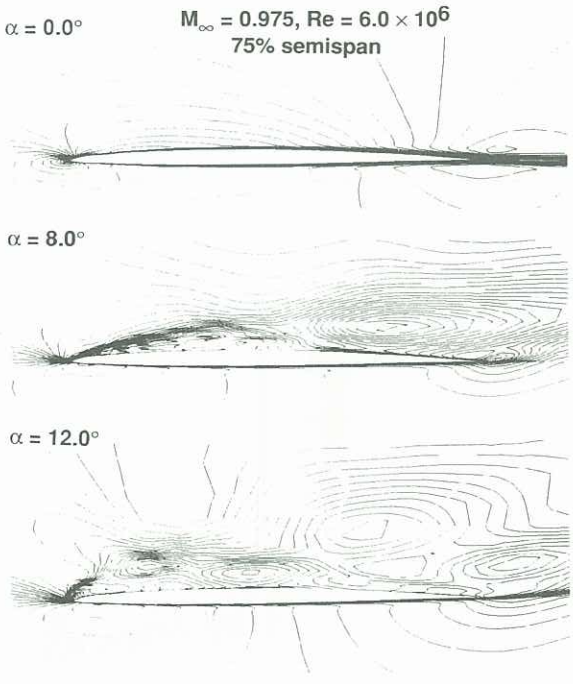

Fig. 4 Density contours at angles of attack of 0.0, 8.0, and 12.0 deg.

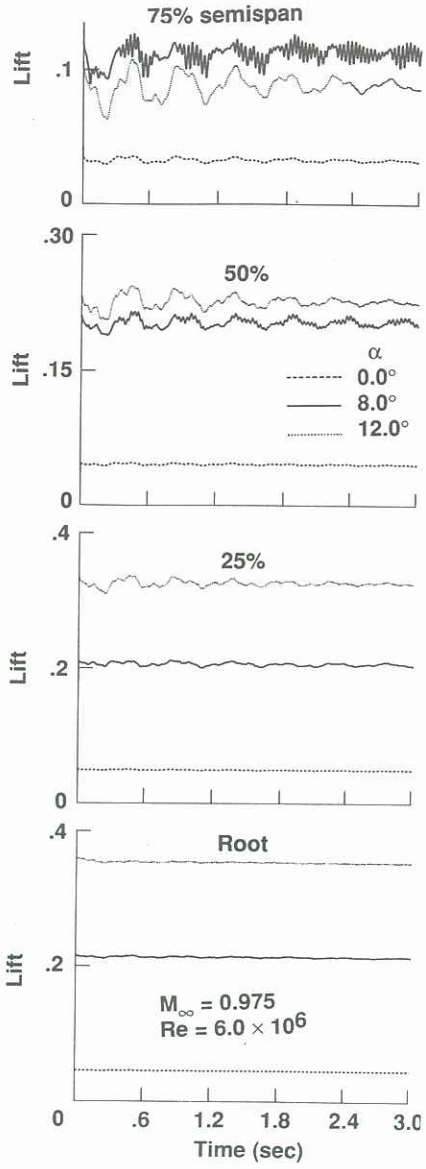

Fig. 5 Unsteady lift responses at angles of attack of 0.0, 8.0, and 12.0 deg.

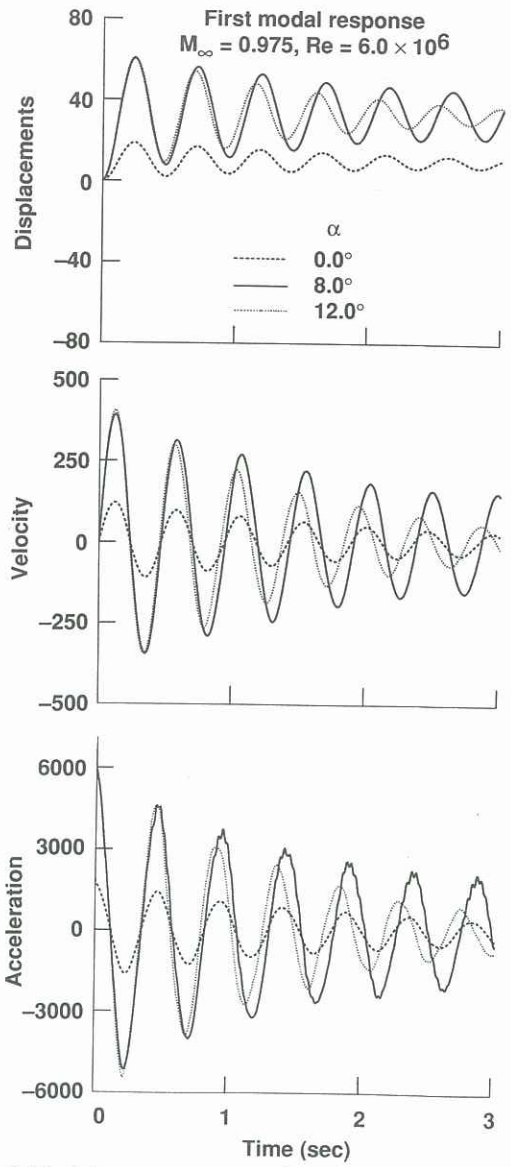

Fig. 6 Modal responses at angles of attack of 0.0, 8.0, and 12.0 deg.

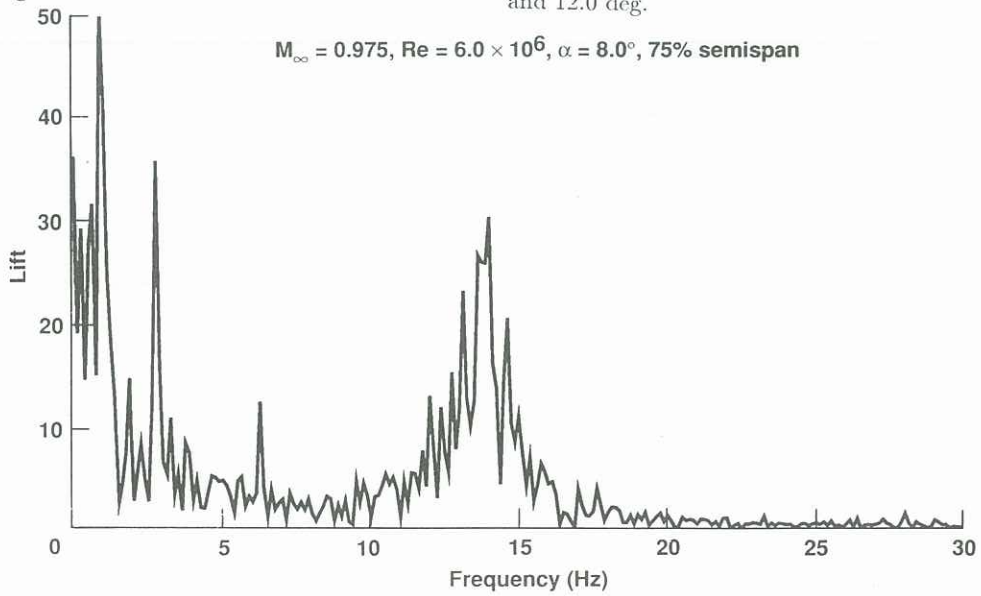

Fig. 7 Fourier analysis results of sectional lift at 8.0 deg angle of attack.